sciendo

Nordic Concrete Federation

© Article authors. This is an open access article distributed under the Creative Commons Attribution-NonCommercial-NoDerivs licens. (http://creaticecommons.org/licenses/by.nc-nd/3.0/).

ISSN online 2545-2819
ISSN print 0800-6377

DOI: 10.2478/ncr-2023-0016

Received: Dec. 15, 2023
Revision: June 12, 2024
Accepted: June 17, 2024

Frost-salt Testing Non-air Entrained High-performance Fly-ash Concrete Part II: Parameter Study of Effect of Internal Cracking on Glue Spall Stress

Iman Asadi, Senior Postdoc researcher, PhD
University for Continuing Education Krems,
Department of Knowledge and Communication Management,
Krems an der Donau, Austria.
iman.asadi@donau-uni.ac.at
Ola Skjølsvold, Senior Researcher, MSc
Department of Architecture, Materials, and structures,
SINTEF Community
Strindvegen 4, Trondheim, Norway
Terje Kanstad, Professor, PhD
Norwegian University of Science and Technology,
Department of Structural Engineering,
Richard Birkelands vei 1A, 7034 Trondheim, Norway
E-mail: terje.kanstad@ntnu.no
Stefan Jacobsen, Professor, PhD
Norwegian University of Science and Technology,
Department of Structural Engineering,
Richard Birkelands vei 1A, 7034 Trondheim, Norway
E-mail: stefan.jacobsen@ntnu.no

ABSTRACT

A parametric analysis of glue spall stress (concrete surface tensile stress at ice-discontinuities by differential thermal expansion ice-concrete) as affected by internal cracking in concrete in the CEN/TS 12390-9 salt-frost slab-test was made. Increasing differential thermal expansion ice-concrete ($\Delta\alpha$) and reduced E-modulus and Poisson ratio (ν) due to internal cracking were used based on data from Part 1 of this study. For the concrete specimens in Part 1 of this study [1] glue spall stress increased by 14 % due to internal cracking whereas reduced ice thickness of 1 – 2 mm due to accelerated Liquid Uptake (LU) in wet freeze/thaw reduced glue spall stress by 34 to 65 %. LU should hence be accounted for in modelling scaling, both due to reduced ice thickness and increased $\Delta\alpha$ due to internal cracking. Increased crack penetration depth and its effect on scaled particle size due to internal cracking were also analyzed.

Keywords: Non-air entrained High performance low carbon concrete, Freeze-thaw, Internal damage, Glue spall stress analysis.

1. INTRODUCTION

In Part 1 of this study [1] frost test performance was studied on low carbon high strength concrete qualities for prospect future bridges in the new ferryboat-free coastal highway in Norway. The service life relates directly to sustainability because all environmental burdens (emissions, consumption of primary raw materials and energy etc.) must be calculated per unit time of service of the structure. Concrete structures are exposed to deteriorating mechanisms that affect service life (reinforcement corrosion, ASR, frost, leaching, sulfate attack, abrasion etc.). In the northern hemisphere freeze-thaw and deicing salt surface scaling attack are important due to the widespread use of deicing chemicals on roads, bridges, parking lots, airfields etc., and due to the tidal zones of marine concrete. The deicer salt scaling is challenging but both the visible scaling and the invisible volumetric damage, termed internal cracking, should be considered [2, 3]. Today adequate service life is ensured by selecting standard "Durability class" depending on standard "Exposure class". Mass-ratio, air entrainment, type of binder and curing are the central material parameters for making frost durable concrete. In [4] Exposure classes XF3/XF4 ("freezing with high saturation without/with salt") specify durability classes MF45/MF40 = effective mass-ratio 0.45/0.40 with air entrainment (≈ 4.5 vol-%). A protective air void system needs high air void specific surface (≈ 30 mm^{-1}) and low air void spacing factor L (≈0.2 mm or less) as quantified by ASTM C457 [5]. The limits depend on the details of the exposure and the concrete material (mass-ratio, type of binder and curing conditions). Air entrainment is, however, a hassle in concrete production with SCMs. Developing frost durable SCM-concrete without air entrainment is therefore desirable. This requires field experience, laboratory testing and/or various other types of experiments. In addition, of course quantitative models are needed based on understanding of the mechanism(s) acting when a de-icing solution is freezing on a concrete surface. The mechanism amplifying concrete surface damage by deicing salts, the pessimum effect with salt and the protective effect of air voids were explained by Valenza and Scherer and Sun and Scherer by the glue spall model [6-8]. Glue spall stress in the concrete surface parallel to the ice-interface (σ_{gs}) is, according to them, due to thermal expansion mismatch compressing the concrete under the ice but causing tensile stress in the concrete surface at gaps or flaws in the ice, Eq.(1) [6-8]:

$$\sigma_{gs} = \left(\frac{E_c}{1-\vartheta_c}\right)\left[\Delta\alpha\Delta T - \sigma_i\left(\frac{1-\vartheta_i}{E_i}\right)\right] \quad (1)$$

In Eq. (1) E_c and E_i are the elastic moduli of concrete and ice, ϑ_c and ϑ_i are the Poisson's ratios of concrete and ice, $\Delta\alpha$ is the difference between the thermal expansion coefficient of ice and concrete, $\Delta\alpha = \alpha_i - \alpha_c = 4.1 * 10^{-5}$ °C^{-1} in this work with $\alpha_i = 5.1 \cdot 10^{-5}$ and $\alpha_c = 1 \cdot 10^{-5}$ °C^{-1} and σ_i is the stress of ice according to eq.(2) [6-8]:

$$\sigma_i = \frac{0.5t_c\left[\frac{E_c}{1-\vartheta_c}\right]\Delta\alpha\Delta T}{0.5t_c\left(\frac{E_c}{E_i}\right)\left[\frac{1-\vartheta_i}{1-\vartheta_c}\right] + t_i} \text{ and } \sigma_c = -2\sigma_i\left(\frac{t_i}{t_c}\right) \quad (2)$$

In Eq. (2) t_c and t_i are the thickness of concrete and ice. High tensile stress in the concrete surface develops at flaws, gaps, cracks, or ice-brine pockets in the ice, initiating and propagating fracture into the concrete. The model explains salt scaling damage: both the characteristic pessimal effect

with maximum scaling damage at moderate deicing salt concentration of around 3 % and the protective effect of air entrainment. Quite different types of experiments [9-11] showed that de-icer salt scaling increases with increasing ice layer thickness as expected from Eqs. (1) and (2). Çopuroğlu and Schlangen [10] in addition developed a numerical model from the Delft lattice model simulating ice cracking during freezing and that cracks could propagate into the concrete initiating scaling. The protective effect of air voids in the glue spall model is to reduce thermal expansion mismatch according to Sun and Scherer [8] since air-voids compress concrete when freezing while highly saturated due to cryo-suction. The powerful suction was observed in freeze-warping of concrete-steel composites with steel on top of capillary saturated air entrained concrete [12]. Air entrained concrete warped convex, opposite of the concave warping without air voids [12]. A recent numerical study by Bahafid et al [13] verified how discontinuities (like cracks, gaps, flaws or brine pockets) in ice on a (non-air entrained) concrete surface gave high local concrete surface tensile stresses in varying combinations of ice- thickness and -gap width during freezing. Tensile stresses increased in the concrete at flaws in the ice, with increasing ice thickness and when the flaws (or gaps) between adjacent ice islands on the concrete surface became narrower. Maximum concrete surface tensile stress always occurred under the ice gaps and was large enough to fracture concrete like in [7, 14].

There are some important similarities between internal cracking and salt scaling during frost exposure. Entrained air voids protect concrete against both cracking and scaling. Furthermore, drying/resaturation pre-treatment of hardened concrete, which can increase both ice formation [15] and deicing salt scaling [16] also increases internal damage [12]. Moreover, there is an accelerated Liquid Uptake (LU) both during freeze/thaw with water and with salt solution [17]. However, a much clearer relation LU-internal frost damage is seen than LU-de-icer salt scaling [18]. Still, it was claimed that LU causes salt scaling damage by ice-body growth [19] and by swelling of the cement paste and scaling of thin flakes [20, 21]. Furthermore, the protective effect of air voids against de-icing salt scaling is reduced in severely dried and re-saturated surfaces [22], for never-dried surfaces [23, 24], for surfaces of fly ash concrete with prolonged water curing [18] and after carbonation of slag concrete [25]. The effects [18, 20-25] are not readily explained by the glue spall model, but so far, the glue spall model stands out as a model that can quantify de-icer salt scaling including the pessimal effect. The model can therefore be useful for service life modelling. The scope of this study, which is a continuation of [1], is therefore to study the glue spall model's capability of quantifying salt-frost degradation rate of concrete with SCMs without air entrainment. Specifically, we investigate how the glue spall stress is affected by simultaneous internal cracking. Surface scaling (oven dried mass loss - kg/m^2), internal cracking (length change – $\Delta L/L$) and LU (weighing including compensation for loss of scaled mass and its evaporable water) were monitored during freeze/thaw slab testing with 3 % NaCl-solution on the concrete surface in [1]. Here, we use those experimental data in a parametric study of the effect of internal cracking on glue spall stress.

2. MATERIALS AND EXPERIMENTS: CONCRETE MIXES AND FROST TESTING

Details are given in part 1 [1]. First the particle packing of the mixed natural-crushed granitic aggregate from Årdal Norway (0-8 mm sand and 8-16 mm coarse with 0.4 % absorption) was maximized. Minimum bulk aggregate void space was measured to be ≈300 liters/ m^3 bulk aggregate by varying the ratio sand/coarse. Workability was then optimized using 335 liters of filler modified cement paste per m^3 concrete with the most dense-packed aggregate mix. Co-polymer water reducer dosage was adapted to give stable fresh concrete mixes with high workability. The main binder was Anlegg FA cement (CEM IIA-V-42.5N) from Heidelberg,

Norway with 75.5% clinker, 15 % fly ash ground with the clinker, 5.5% gypsum, and 4% limestone filler. A dry condensed silica fume from Elkem, Norway and additional low lime Fly ash were also used. Four final concrete mixes were prepared and all data are given in Part 1 of this work [1]. Fresh air void contents were 1.4 – 1.9 vol-% and 91-day compressive strengths > 100 MPa for all four mixes. Environmental performance indicators were calculated with an LCA-tool used by the Norwegian ready mixed concrete industry. Mix 2 had lowest Global Warming Potential (GWP) from cradle to gate according to relevant ISO- and EN-standards with GWP ≈ 200 kg/m^3 almost giving the rating "Low carbon extreme" in the Norwegian Concrete Association's environmental performance classification scheme [26].

Frost testing was done on ≈5 x 15 x 15 cm slabs cut from 15 cm cubes [27] with three types of curing. *Normal:* Cubes stored 7d in water and 14 d in the climate room (at 65%RH, 20 °C, 45 g/m^2·h evaporation rate from free water surface). Then the cubes were sawn into 47 mm thick slabs and further 7d exposure in the climate room while prepared with non-absorptive butyl tape to make the dam and then + 3d with pure water on the test surface. Then water was replaced with 3 mm 3 % NaCl solution before freeze/thaw testing for 56 cycles. *Dried*: Cubes stored 7d in water, 14 d in the same climate room, then sawing and further 14 weeks exposure in the climate room, prepared with butyl tape, and then 3d with pure water on the test surface. Then water was replaced with 3 mm 3 % NaCl solution before freeze/thaw testing for 112 cycles. *Wrapped:* Cubes stored 7d in water, 14d in the same climate room, sawing, and 14 weeks packed in plastic-covered aluminum foil, then prepared with butyl tape before 3d with pure water on the surface. Then water was replaced with 3mm 3 % NaCl solution, before freeze/thaw testing for 112 cycles. During frost-deicing testing of the 3 x 16 slabs measurements were made of scaling of concrete from the top surface (kg/m^2). Internal damage was measured as length change horizontally when thawed at 20 °C across the 15 cm width of 2 of 4 parallel slabs using a dilatometer on invar studs drilled and glued into the 47 mm thick vertical slab surfaces at half-height and mid-width. LU was monitored by weighing slabs in SSD state with the non-absorptive butyl after each scaling- and length measurement and adding scaled mass corrected for loss of evaporable water.

3 RESULTS AND DISCUSSION

3.1 Freeze/thaw results and relation to penetration of salt solution

Table 4 in part 1 [1] shows that Mix 1 is quite scaling resistant after Normal and Dried curing. Common accept criteria of the test are $m_{56} < 0.5$ or $m_{56} < 1$ kg/m^2 and acceleration factor (m_{56}/m_{28}) < 2. Mix 2 – 4 and Wrapped curing perform less well. There are several Wrapped mixes that have quite low scaling m_{56}, but the acceleration is highest in Wrapped curing, so all these mixes fail, see Figure 3 in [1] and the (m_{56}/m_{28}) and (m_{112}/m_{56}) acceleration factors in Table 4 in [1].

The measurements of internal damage in part 1 [1] showed that all specimens had internal damage with expansive strain > 0.001 already after 28 cycles, i.e. > approximately 10 times the tensile fracture strain of concrete. Strain increased at continued cycling. One mix had expansion > 0.01 (= 1%!) after 56 cycles and at least 6 mixes had expansion > 0.01 after 112 cycles, see Figure 4 in [1]. There was a tendency that also development of internal damage was more accelerated after wrapped curing, just like the acceleration of scaling, see Table 5 in [1].

The measurements of Liquid Uptake (LU) during freeze/thaw were in line with previous experience [7]: LU correlates clearly to Internal damage and a bit less clearly to scaling.

During frost salt scaling testing, it was observed that salt solution could penetrate through the samples to varying degrees, typically starting at/around 28-42 cycles on those specimens with the most extreme penetration. Table 1 gives an overview of observations of the presence of salt solution on the test surfaces during freezing and thawing. From the table, leakage starts earliest for the Dried cure samples: 28 – 42 cycles. For the Wrapped cure, there was slight leakage of salt solution until 84-98 cycles for Mix1, whereas Mix 2 – 4 had leakage somewhat earlier. Some of the specimens with high leakage were stopped as leakage became too severe. The experiences at our lab with the preparation method used with Butyl tape are very good, with clearly less leakage between concrete and rubber compared to previous types of rubber glued with other types of glue [28]. In addition, the butyl is non-absorptive so that LU can be measured. The leakages observed in table 1 were hence mainly through the concrete and could be seen since the bottom of the concrete slab was not covered. The bond between concrete and butyl rubber only became affected in specimens with the most severe scaling.

Table 1 - Leakage visualization

Sample ID	Curing Conditions	Visual observations at different cycles								
		7	14	28	42	56	70	84	98	112
Mix 1	Normal	NL	NL	NL	NL	NL	*			
	Dried	NL	NL	NL	1 NL, 3ML	1 NL, 3ML	ML	L	L	L
	Wrapped	NL	NL	NL	NL	NL	NL	NL	2NL 2L	1NL3 L
Mix 2	Normal	NL	NL	NL	1L, 3NL	L	*			
	Dried	NL	NL	NL	L	L	L	L	L	L
	Wrapped	NL	NL	NL	NL	3NL, 1L	1ML,3 L	L	L	L
Mix 3	Normal	NL	NL	NL	NL	NL	*			
	Dried	NL	NL	NL	2NL,2L	L	L	L	L	L
	Wrapped	NL	NL	NL	NL	3NL, 1L	L	L	L	L
Mix 4	Normal	NL	NL	NL	NL	1L, 3NL	*			
	Dried	NL	NL	L	L	L	L	L	L	L
	Wrapped	NL	NL	NL	NL	ML	L	L	L	L

NL: No Leakage: 3 mm NaCl on the surface, ML: Mild Leakage: less than 3 mm NaCl on the surface, L: Leakage: no NaCl on the surface
*: Normal cure only run to 56 cycles

Figure 1 shows scaling at individual cycles, or frequency of scaling, versus the number of freeze-thaw cycles. The plots show the intensity of the scaling as the number of freeze-thaw cycles increases. For Normal curing conditions and Wrapped curing conditions, scaling reaches a plateau or accelerates throughout the cycling. In contrast, there are clear peaks in cycling at an early stage, around 7 – 28 cycles for Dried curing conditions. This illustrates how Drying-preconditioning presumably increases the flow of liquid through the concrete during freeze-thaw compared to the other two forms of curing conditions with less/no drying. The plots in this figure can be interpreted based on the visual observations of samples, as summarized in Table 1 above here.

Regarding Mix 1 (030AnlFA), we observed mild leakages on the surface of samples under Dried curing conditions at the 42nd cycle. However, for 0.30 FA16SF, we observed the leakage sooner than on the other mixes at the 28th cycle for Dried cure. It also can be seen in Figure 1 that the maximum scaling is at the 7th cycle.

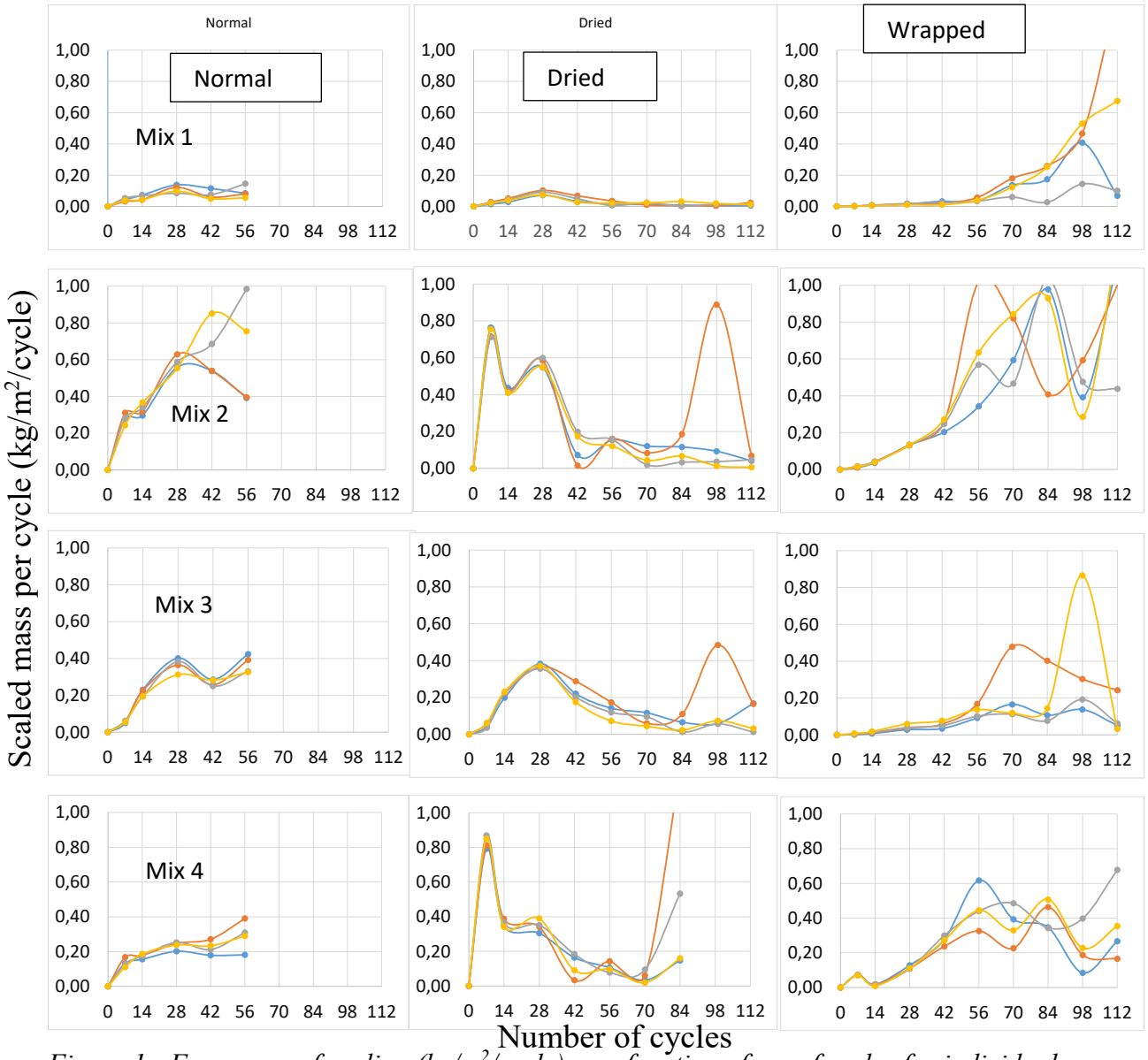

Figure 1 - Frequency of scaling (kg/m²/cycle) as a function of no. of cycles for individual specimens.

Table 1 and Figure 1 show how fluid penetrated the specimens due to internal damage and the variations in scaling per cycle (= frequency of scaling) for the individual slabs. Together, Table 1 and Figure 1 indicate that the reduction of fluid on top of the specimens due to penetration of the bulk of the concrete was most common for Dried curing which also showed largest drop of scaling per cycle. In addition to the correlation LU-internal damage, see also Figure 7 in part 1 [1], there is a clear effect of LU on ice thickness, see further below.

3.2 Parameter studies of glue spall stress in concrete with internal cracking

The concrete material parameters of Eqs. (1) and (2) are affected by internal cracking and by LU. A parametric study was therefore performed of the resulting effect on σ_{gs}. Since LU can become very high the ice thickness will decrease during freeze/thaw so that the glue spall stress will decrease, Eqs. (1) and (2). LU = 1 kg/m² means ice thickness reduction ≈1 mm. From Figure 6 in Part 1 [1] it is seen that LU after 56 cycles often was much higher: typically, around 2 kg/m², but

also higher than that. There could hence be a marked reduction of ice thickness corresponding to the LU. At the same time internal cracking increased the residual expansion, increasing the differential thermal expansion $\Delta\alpha$.

The thermal expansion coefficients of ice and undamaged concrete in Eqs.(1) and (2) are: $\alpha_i = 5.1 \cdot 10^{-5}$ and $\alpha_c = 1 \cdot 10^{-5}$ °C^{-1}, respectively. α_i we assume constant [29]. However, α_c during freezing with internal frost damage is reduced compared to in undamaged concrete due to the expansion during freezing and resulting increase of residual expansion in each cycle (Figure 4 in Part 1). We therefore estimate the net reduction of α_c as the amount of net residual thermal expansion for each cycle distributed over a temperature difference from 0 to -20 °C. We know from experience, for example Ref. [28], that the thermal expansion of concrete is not constant during the freezing thawing process. There can be expansion or contraction in the concrete above and below the linear thermal expansion coefficient during the freezing/thawing cycle resulting in some residual length change after each completed freeze/thaw cycle. Since we here only measured residual expansion at 20 °C at the end of each freeze/thaw cycle, we used this value to calculate net reduction of α_c due to freezing, or more precisely due to internal frost damage. This was done by assuming that the observed net expansion per cycle took place during freezing only, i.e over a temperature drop from 0 to -20 °C, i.e. $\Delta T = 20$ °C. Figure 2 shows plots of this net reduction of α_c simply obtained by dividing residual expansion per cycle by $\Delta T = 20$ °C. This expansion during freezing therefore resulted in gradual reductions of concrete thermal expansion coefficients, α_c, of $0.5 - 0.9 \cdot 10^{-5}$ °C^{-1}. Figure 2 shows an example of net reduction of concrete thermal expansion coefficient as average of all mixes with dried curing.

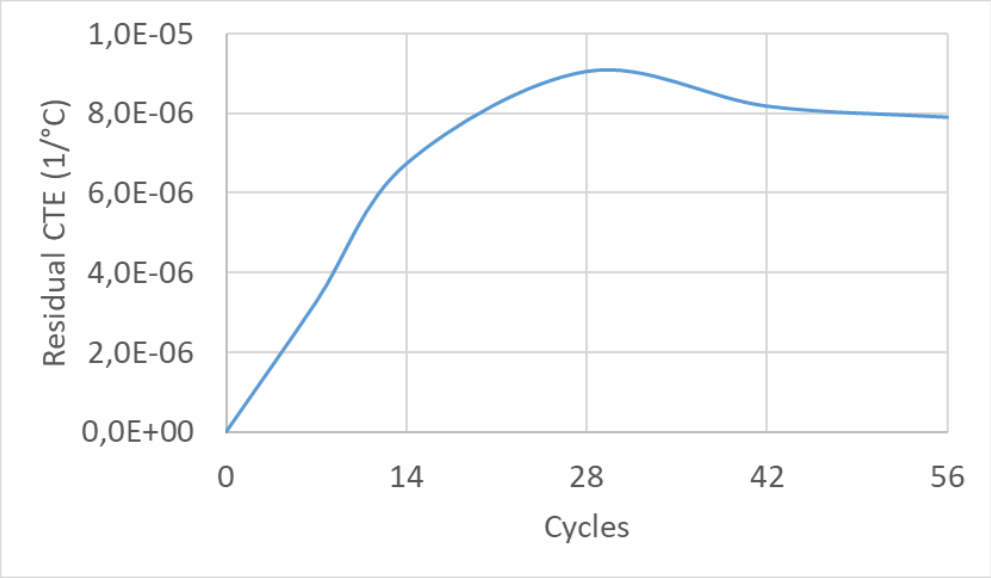

Figure 2 - Net reduction of α_c = Coefficient of Thermal Expansion (CTE) due to internal cracking – average all 4 mixes with dried curing.

This net reduction of α_c again lead to a corresponding increase of $\Delta\alpha = \alpha_i - \alpha_c$ from undamaged to frost damaged concrete: from $\Delta\alpha_{undamaged} = (5.1 \cdot 10^{-5} - 1 \cdot 10^{-5}) = 4.1 \cdot 10^{-5}$ °C^{-1} to $\Delta\alpha_{max,frostdamaged} = (5.1 \cdot 10^{-5} - 1 \cdot 10^{-5} + 0.9 \cdot 10^{-5}) = 5 \cdot 10^{-5}$ °C^{-1} . The maximum value occurs at 28 cycles for the concretes with dried curing, see Figure 2. The maximum value of $\Delta\alpha$ calculated in this way is a conservative estimate for $\Delta\alpha$. Continuous measurements of dilatometry during entire freeze/thaw cycles often show larger expansion than the residual expansion we measured on our slabs at +20

°C, for example at primary ice formation just below 0°C. In our parameter studies below, we used $\Delta\alpha = 4.6\text{-}4.7 \cdot 10^{-5}$ °C^{-} at 28 and 56 cycles based on averages, see Figure 4a right hand y-axis.

The Poisson ratio of the concrete will be reduced by the internal cracking. Ice contracting on cooling will cause strain parallel to the concrete surface that will tend to close concrete cracks without affecting lateral strain at severe internal cracking. Hence, ϑ_c is likely close to zero already at 28 cycles in our concrete specimens. E-modulus drops by the internal cracking and was calculated from measured strain and a model previously developed at our department for drop of E-modulus for concrete cracked due to ASR [30].

Figure 3a shows E-modulus as function of strain during freeze/thaw calculated as average for all 4 mixes and 3 curing conditions shown in Figure 4 in [1]. Figure 3b shows the evolution of glue spall stress on the left-hand y-axis as function of number of freeze/thaw cycles. The E-modulus is based on Figure 3a. However, ice thickness is varying as discussed above due to LU. Up to 28 cycles the ice thickness is 3 mm whereas after 28 cycles two different reductions of ice thickness are used: 1 mm and 2 mm. The right-hand y-axis of Figure 3b shows the trend of scaling frequencies based on Figure 1 in this paper.

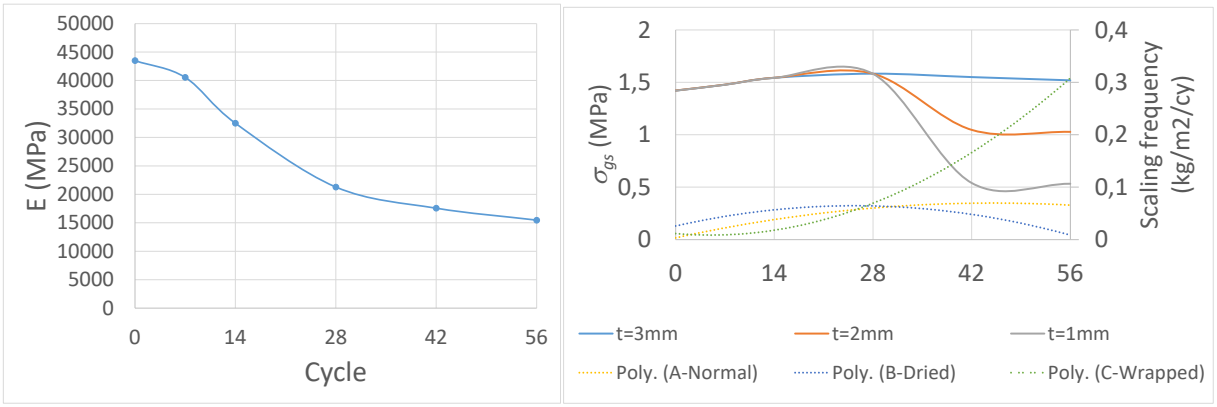

a) b)

Figure 3 - a) concrete E-modulus, and b) glue spall stress at varying ice thickness and polynomial trend of scaling frequency, average 4 mixes, each with 3 curing conditions (Thermal expansion differences and E-mod vs no of cycles based on measured strain (Fig. 2) and [30])

The right-hand axis of Figure 3b shows average polynomial trend of scaling frequency for the 4 mixes for each of the 3 types of curing. The results are based on Figure 1 in this paper (and Table 4 and Figure 3 in [1]) and show linear, accelerated, and decelerated scaling progress for Normal, Wrapped and Dried curing, respectively. The Wrapped curing also had the largest tendency to acceleration of internal damage, so it is possible that internal cracking in this case had a direct influence on scaling. Figure 4 shows more parameter studies on effect of ice thickness, coefficient of thermal expansion and poisson ratio on glue spall stress.

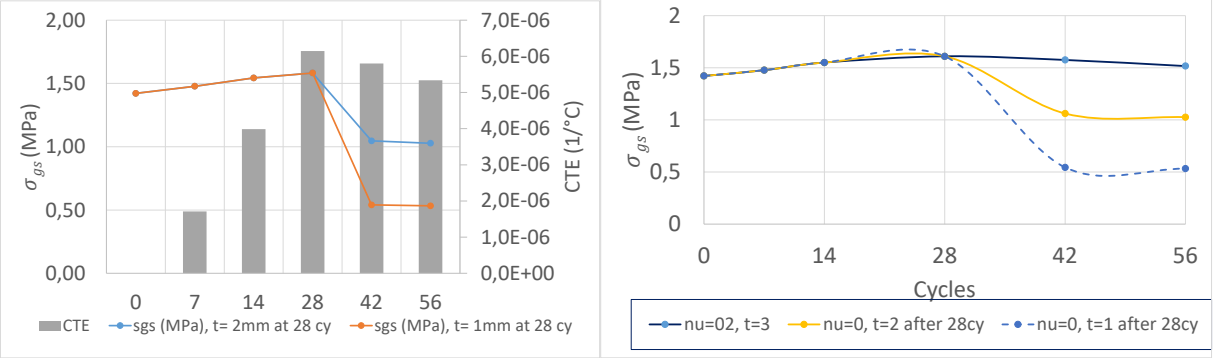

a) b)

Figure 4 - a) Glue spall stress (σ_{gs}) with CTE vs. no of cycles, b) Glue spall stress vs. no of cycles with Poisson ratio 0 and 0.2. Both: drop of ice thickness after 28 cycles.

Figure 3b and 4 focus on the effect of ice thickness on glue spall stress due to the high LU at high internal cracking. Such cracking with high penetration of fluid must be reported specifically according to [27] and, as mentioned, was not caused by leakage between concrete and butyl-tape in this work but due to penetration of bulk concrete.

In sum Figures 3b and 4 show that before 28 cycles when ice thickness is still 3 mm there is a moderate increase of 14 % of glue spall stress by internal frost damage due to drop of modulus of elasticity, Poisson's ratio, and concrete fracture energy. At 28 cycles, as ice thickness is reduced to either 2 or 1 mm corresponding to LU of 1 and 2 kg/m^2 the drop of glue spall stress is much larger: 34 - 65 %.

3.3 Parameter studies of depth of penetration of fracture of scaled material

A study of shape and size of concrete particles scaled from surfaces during frost testing was previously done at our lab [31]. It was observed that the relative particle Thickness 2T/(W+L) was lower, and the particle size (W+L)/2 was more uniform for particles from the salt scaling test than for particles from the rapid freeze/thaw test in water. We therefore estimate scaling depth as a relative crack penetration depth by the fracture mechanics of the glue spall model [11, 14] applying the relation Dunder's parameter (β), relative fracture energy (Γ_c/Γ_i) and determining crack penetration depth d/t_f (d: crack depth, t_f: film- or ice thickness). The main analysis and results are given below in Figure 5 showing crack penetration depth vs number of frost cycles. The parameters and crack depths are also given in Table 2.

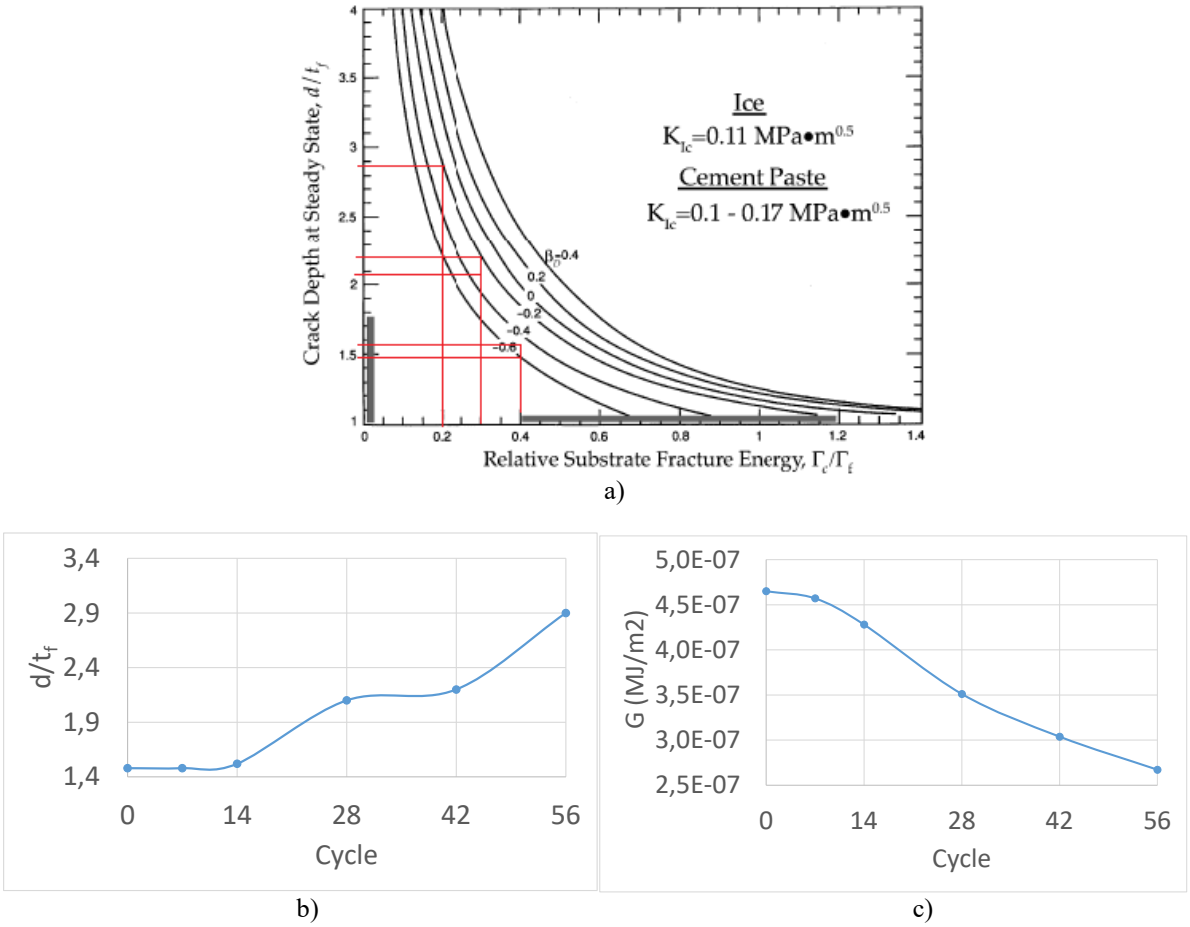

Figure 5 - a) Finding crack depth based on relative fracture energy, and β, figure reproduced from [14], b) relative crack depth d/t_f and c) relative fracture energy vs. no of cycles

The parameter studies of relative crack penetration depth show (last row of table 2) that relative thickness (d/t_f) increases when there is large internal damage in the concrete.

Table 2 - Parameter variation and effect of internal frost damage in glue spall analysis

Parameter	No damage	Internal damage 28/56 cy
E-modulus E	43.5 GPa	21.2/15.4 GPa
Poisson ratio ν	0.2	0*
Increased thermal expansion ERCTE	0	6.15E-06/5.34E-06
Differential thermal expansion Δα	4.1E-05	4.7E-05/4.6E-05**
Relative crack depth d/t_f	1.42	2.1/2.9

*: closing of cracks, no lateral dilation, **: increase due to expansion by internal frost damage

The drop of glue spall stress seen from 28 to 56 cycles in Figures 3b and 4 when ice thickness is reduced should be seen together with Figure 5 and Table 2. This indicates that the effect of internal damage is a doubling of the thickness of the scaled particles. The relative thickness (d/t_f) = 1.4 – 2.9 gives absolute ice thickness = 4.2 – 8.7 mm. These values are higher than observed by Valenza and Scherer (2006) who calculated scaling thickness = 0.75 times ice thickness = 2.25 mm without any internal damage. This is also high compared to the observation in [31] of maximum ≈1 mm thickness after 5 - 7 cycles of both air entrained and non-air entrained w/b = 0.40 concrete with sawn surfaces. At higher number of cycles and more damage, 3 – 5 mm max thickness were observed which also included larger aggregate particles. The scatter in size and thickness were,

however, large and particle size distributions in [31] indicated mean size in the range 0.5 – 1 mm. So, with 2T/(L+W) = 0.2 this indicates mean thickness in the order 0.1 – 0.2 mm. Hence, the calculated thickness is in the same order of magnitude as observed maximum thickness whereas average observed thickness is lower than calculated by the above fracture mechanics approach.

In a recent study by Maus et al [29] CT-scanning revealed that the saline ice on the concrete surface is micro-columnar and permeable. Hence, both glue spall stress and LU during freeze/thaw should be modelled with this kind of defect and permeable ice. Permeable ice would significantly affect the modelling of LU in deicer salt scaling compared to the zero-flow assumed through fresh water ice in [32]. Also, the loss of protective effect of air voids after prolonged water curing of FA-concrete, after severe and no drying, and after carbonation of slag-concrete [18, 20, 25] needs investigation. Internal damage can then affect glue spall stress to different degrees depending on how $\Delta\alpha$ is affected. Another important aspect is water filling of air voids which will affect frost test performance.

Acceleration of scaling and acceleration of strain may be explained by crack filling, but it is not clear why glue spall stress should increase so much more in this case, which happened for specimens with the theoretically best curing condition (prolonged sealed curing without drying). Possibly the prolonged cure caused high degree of saturation in the slowly hydrating fly ash, amplifying internal damage.

4. CONCLUSIONS

Based on the experimental observations of scaling, internal cracking and LU in part 1 [1] and the parameters analyzed here in part 2, glue-spall stress increases on average 14 % from 0 to 28 cy due to internal cracking. This is due to increased $\Delta\alpha$ from residual expansion after each cycle and in spite of reduced E_c (strain-based model [28]) and assumed reduced ν_c. The Liquid Uptake (LU) during freeze/thaw reduces ice thickness and causes water-/ice filling of cracks. 1-2 mm ice thickness reduction has larger effect on glue spall stress: (-34 to -65 %) than the severe internal cracking has with increase of $\Delta\alpha$ and drop of E and ν: (+14%).

Simultaneous internal cracking and surface scaling will cause shorter service life due to thicker scaled particles. The fracture mechanics method of the glue spall model for estimation of crack penetration depth indicates that the thickness of the scaling can be doubled by the severe internal cracking in our specimens, though the calculated thickness is larger than average thickness observed in experiments. Some qualitative assessments based on the observations in part 1 [1] on the progress of scaling are:

- Deceleration of scaling is presumably caused by reduced ice thickness due to penetration of solution in cracked concrete causing high LU. This supports glue spall – internal cracking interaction.
- Acceleration of scaling and acceleration of strain may be explained by crack filling, but it is not clear why glue spall stress should increase so much more in this case, which happened for specimens with the theoretically best curing condition (prolonged sealed curing). Possibly this caused high degree of saturation, amplifying internal damage.

ACKNOWLEDGMENTS

The work was funded by Norwegian Road Administration, Ferry-free E39-project and NTNU SO-project no 81618007 at the Department of Structural Engineering.

REFERENCES

1. Asadi I, Skjølsvold O., Kanstad T., Jacobsen S. Frost-salt testing non-air entrained high-performance fly-ash concrete. Part I: Relations liquid uptake - internal cracking – scaling, submitted to NCR.
2. Skripkiūnas G, Nagrockienė D, Girskas G, Vaičienė M & Baranauskaitė : " The cement type effect on freeze–thaw and deicing salt resistance of concrete ". *Procedia engineering*, *57*, 2013, pp.1045-1051.
3. Zhao J, Cai G, Gao D & Zhao S : "Influences of freeze–thaw cycle and curing time on chloride ion penetration resistance of Sulphoaluminate cement concrete". *Construction and Building Materials*, 2014. **53**: pp. 305-311
4. EN 206. BSI Standards Publication Concrete : "Specification, performance, production and conformity". Br Stand 2013:30.
5. ASTM International. (2016). Standard Test Method for Microscopical Determination of Parameters of the Air-Void System in Hardened Concrete: C 457/C 457M-12. ASTM.6.
6. Valenza II, John J & George W. Scherer : "A review of salt scaling: I. Phenomenology. " *Cement and Concrete Research* 37.7 (2007): pp.1007-1021
7. Valenza II, John J & George W. Scherer : "A review of salt scaling: II. Mechanisms. " *Cement and Concrete Research* 37.7 (2007):pp. 1022-1034.
8. Sun Z & Scherer GW : "Effect of air voids on salt scaling and internal freezing". *Cement and Concrete Research*, 2010. **40**(2): pp. 260-270.
9. Faheem A : "Influence of thermal boundary conditions and temperature distribution in concrete on frost scaling–experimental and numerical study"., PhD, DTU (2021) 158 p.
10. Çopuroğlu O & Schlangen E : "Modeling of frost salt scaling". *Cement and Concrete Research*, 2008. **38**(1): pp. 27-39.
11. Tremblay MH, Lory F, Marchand J, Scherer GW & Valenza JJ : "Ability of the glue spall model to account for the de-icer salt scaling deterioration of concrete". Paper W4-07.3 in proceedings of 12th ICCC. National Research Council of Canada, Montreal, Canada, 2007.
12. Jacobsen S & Scherer GW : "Freezing induced stresses in concrete-steel composite beams and effect of air voids". in I: *Proceedings* of the International RILEM Conference Materials, Systems and Structures in Civil Engineering 2016 Segment on Frost Action in Concrete. Rilem publications. 2016.
13. Bahafid S, Hendriks M, Jacobsen S & Geiker M : "Revisiting concrete frost salt scaling: On the role of the frozen salt solution micro-structure". *Cement and Concrete Research*, 2022. **157**, 106803.
14. Valenza JJ & Scherer GW : "Mechanism for salt scaling". *Journal of the American Ceramic Society*, 2006. **89**(4): pp. 1161-1179.
15. Bager DH & Sellevold EJ : "Ice formation in hardened cement paste, part I—Room temperature cured pastes with variable moisture contents". *Cement and Concrete Research*, 1986. **16**(5): p. 709-720.

16. Bager DH & Sellevold EJ : "Ice formation in hardened cement paste, Part II—drying and resaturation on room temperature cured pastes". *Cement and Concrete Research*, 1986. **16**(6): pp. 835-844.
17. Jacobsen S, Asadi I, Skjøsvold O & Kanstad T : "Frost testing non-air entrained SCM HPC: salt-scaling and internal damage". Rilem week, Vancouver, Canada, 2023, 8 p.
18. Shpak A, Gong F & Jacobsen S: "Frost durability of high-volume fly ash concrete: Relation liquid transport-damage". *Cement and Concrete Research*, 2023. **163**, 107017.
19. Lindmark S : "Mechanisms of salt frost scaling of Portland cement-bound materials: Studies and hypothesis". 1998, Lund University, Report TVBM 1017, 266 p.
20. Liu Z & Hansen W : "Freezing characteristics of air-entrained concrete in the presence of deicing salt". *Cement and Concrete Research*, 2015. **74**: pp. 10-18.
21. Liu Z, Hansen W & Wang F : "Pumping effect to accelerate liquid uptake in concrete and its implications on salt frost durability". *Construction and building materials*, 2018. **158**: pp. 181-188.
22. Sellevold E & Farstad T.: *Nordic Concrete Research.* Publ. No 10, 1991: p. 121-138.
23. Verbeck GJ & Klieger P : "Studies of'salt'scaling of concrete". *Highway Research Board Bulletin*, 1957(150).
24. Jacobsen S, Marchand J, Boisvert L, Pigeon M & Sellevold EJ : "Frost deicer salt scaling testing of concrete: effect of drying and natural weathering". *Cement Concrete and Aggregates*, 1997. **19**: pp. 8-16.
25. Utgenannt P : "The influence of ageing on the salt-frost resistance of concrete". Lund University Report TVBM 1021. 2004, 346 p + 11 app.
26. *NB Publikasjon 37 Lavkarbonbetong (Norw Conc Ass Publ 37 Low carbon concrete) 2020, 37 pages*
27. Technical Specification (CN/TS): "Testing hardened concrete – part 9: Freeze-thaw resistance with de-icing salts, Scaling". CEN/TS 12390-9:2016.
28. Shpak A : "Production and documentation of frost durable high-volume fly ash concrete: air entrainment, cracking and scaling in performance testing". Ph.D Thesis 2020:366, Norwegian University of Science and Technology (NTNU) 2020,
29. Maus S, Bahafid S, Hendriks M, Jacobsen S & Geiker MR: "X-ray micro-tomographic imaging and modelling of saline ice properties in concrete frost salt scaling experiments". *Cold Regions Science and Technology*, 2023. **208**, 103780.
30. Kongshaug SS, Oseland O, Kanstad T, Hendriks MA, Rodum E & Markeset G: "Experimental investigation of ASR-affected concrete–The influence of uniaxial loading on the evolution of mechanical properties, expansion and damage indices". *Construction and Building Materials*, 2020. **245**, 118384.
31. Brun MB, Shpak A & Jacobsen S: "Shape and size of particles scaled from concrete surfaces during salt frost testing and rapid freeze/thaw in water". *Nordic Concrete Research*, 2021. **64**(1): pp. 53-68.
32. Gong F & Jacobsen S: "Modeling of water transport in highly saturated concrete with wet surface during freeze/thaw". *Cement and Concrete Research*, 2019. **115**: pp. 294-307.